International Journal for Innovative Engineering and Management Research
A Peer Revieved Open Access International Journal
www.ijiemr.org

COPY RIGHT

IJIEMR Transactions, online available on 8th Dec2017.Link
:http://www.ijiemr.org/downloads.php?vol=Volume-6&issue=ISSUE-12

Title: **HYBRID GENERATION SCHEME FOR A HIGH STEP-UP DC TO DC CONVERTER WITH INDUCTION MOTOR DRIVE**

Volume 06, Issue 12, Pages: 271–282.
Paper Authors

PADMASETTY.KASI RAO, BOBBADI.ADINARAYANA
A1 Global Institute of Engineering & Technology, Markapur; Prakasam (Dt); A.P, India.

USE THIS BARCODE TO ACCESS YOUR ONLINE PAPER

To Secure Your Paper As Per UGC Guidelines We Are Providing A Electronic Bar Code

International Journal for Innovative Engineering and Management Research
A Peer Revieved Open Access International Journal
www.ijiemr.org

HYBRID GENERATION SCHEME FOR A HIGH STEP-UP DC TO DC CONVERTER WITH INDUCTION MOTOR DRIVE

[1]PADMASETTY.KASI RAO, [2]BOBBADI. ADINARAYANA

[1]Assistant Professor,Department of Electrical & Electronics Engineering,A1 Global Institute of Engineering & Technology, Markapur; Prakasam (Dt); A.P, India.

[2]Assistant Professor,Department of Electrical & Electronics Engineering,A1 Global Institute of Engineering & Technology, Markapur; Prakasam (Dt); A.P, India.

Abstract- This project presents Hybrid renewable energy topology for a high gain boost converter with Induction motor drive applications. Recently renewable energy generation systems are gaining more attraction due to the exhaustive nature of fossil fuel resources and its increased prices. Also the need for pollution free green energy has created a keen interest towards alternate energy sources. DC-DC converters are electronic devices used whenever we want to change DC electrical power efficiently from one voltage level to another. The proposed system advantageous to high voltage conversion gain, small volume, low voltage stress and low conduction loss on switches, as well as the reduced reverse-recovery problem. In this a novel PWM scheme for two-phase interleaved boost converter with voltage multiplier for fuel cell power system by combining APS and traditional interleaving PWM control is proposed. A drive system is typically composed of three components: a dc-dc converter that converts low dc voltages to a required high dc voltage, an inverter that converts the high dc voltage to a single- or three-phase ac voltage, by combining alternating phase shift (APS) control and traditional interleaving PWM control controls the converter operation. In extension the high gain converter is connected to an inverter fed with Induction motor drive. The Induction motor stator current speed and torque responses are studied. The system performance can be analyzed by using MATLAB/SIMULINK software.

Keywords: Hybrid renewable energy system, High-gain converter, PWM control, Induction motor drive.

I. INTRODUCTION

Renewable energy generation systems based on solar photovoltaics and fuel cells (FCs) need to be conditioned for both dc and ac loads. Photovoltaic cells are solid-state semiconductor devices that convert the light energy into electrical energy directly. These cells are usually made of silicon with traces of other elements and are considered as first cousins to transistors, LED's and other electronic devices. The overall system includes power electronics energy conversion technologies and may include energy storage based on the target application. However, the FC systems must be supported through additional energy storage unit to achieve high-quality supply

International Journal for Innovative Engineering and Management Research
A Peer Revieved Open Access International Journal
www.ijiemr.org

of power [1]–[4]. When such systems are used to power ac loads or to be connected with the electricity grid, an inversion stage is also required.

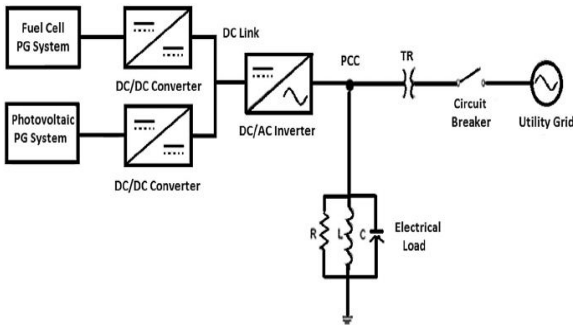

Fig.3.1. Grid-connected power system based on fuel cell

The dc/dc converter will generate a high frequency input current ripple, which will reduce the life time of the fuel cell stack [5]. In addition, the hydrogen energy utilization decreases with increasing the current ripple of the fuel cell stack output. Therefore, the dc/dc converter for the system as shown in Fig.1 should have high step-up ratio with minimum input current ripple.Bidirectional DC DC converters serves the purpose of stepping up or stepping down the voltage level between its input and output along with the capability of power flow in both the directions. Bidirectional DC DC converters have attracted a great deal of applications in the area of the energy storage systems for Hybrid Vehicles , Renewable energy storage systems, Uninterruptable power supplies and Fuel cell storage systems [6]. Traditionally they were used for the motor drives for the speed control and regenerative braking. Bidirectional DC DC converters are employed when the DC bus voltage regulation has to be achieved along with the power flow capability in both the direction.

High step-up ratio can be achieved by combining classical boost converter with switched inductors, coupled inductors, high-frequency transformer or switched capacitor. They can obtain high step-up ratio with high efficiency, low-voltage stress, and low electromagnetic interference [7-8]. In order to reduce output fuel cell stack output current ripple or the dc/dc converter input current ripple, either a passive filter or active filter can be used, however, this will increase the complexity of the system. The high DC-DC converter is used to make proper operation fed with induction motor drive. A DC–DC converter with a high step-up voltage gain is used for several applications, such as high-intensity discharge lamp ballasts for automobile headlamps, fuel cell energy conversion systems, solar-cell energy conversion systems and battery backup systems for uninterruptible power supplies [9]. Theoretically, a dc–dc boost converter can achieve a high step-up voltage gain with an extremely high duty ratioThe converter shown in Fig.2 can achieve low-voltage stress in the power devices, which increases the conversion efficiency. However, this is only true in heavy load when the voltage stress of the power devices might increase when it works in discontinuous conduction mode (DCM), which occurs when fuel cell only supplies a light local load as shown in Fig.1. In this case, higher voltage power devices need to be used, and therefore its cost and power loss will be increased. These authors proposed a new pulse width modulation (PWM) control method, named as alternating phase shift (APS), to

International Journal for Innovative Engineering and Management Research
A Peer Revieved Open Access International Journal
www.ijiemr.org

overcome the problem when the converter operates in light load [10-12].

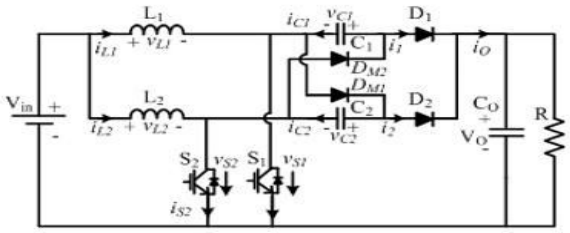

Fig.2. Structure of two-phase interleaved boost converter with voltage multiplier [13], [14]

This project investigates a novel PWM scheme for two-phase interleaved boost converter with voltage multiplier for fuel cell power system by combining APS and traditional interleaving PWM control. The APS control is used to reduce the voltage stress on switches in light load while the traditional interleaving control is used to keep better performance in heavy load. The boundary condition for swapping between APS and traditional interleaving PWM control is derived [13]. Based on the aforementioned analysis, a full power range control combining APS and traditional interleaving control is proposed. Loss breakdown analysis is also given to explore the efficiency of the converter.

II. BOUNDARY CONDITION ANALYSIS WITH TRADITIONAL INTERLEAVING CONTROL FOR LOW POWER OPERATION

It is assumed that all components in the converter are ideal, both capacitor C1 and C2 are large enough, and duty cycle is less than 0.5. The operation of a switching cycle of the converter can be divided into six stages at boundary condition which the voltage stress on switch will be larger than half of the output voltage with traditional interleaving control, as shown in Fig.3. Typical theoretical waveforms at boundary condition are shown in Fig.4.

1) First Stage (t_0,t_1): At the moment of t0, both switch S_1 and S_2 are off, the energy stored in the inductor L_2 and capacitor C_2 in previous stage are transferred to the output capacitor C_O through D_2 as shown in Fig.3(a). The voltage stress on switch S1 is the input voltage Vin, and the voltage stress on switch S_2 is ($V_O - V_{C2}$), where VO is the output voltage and V_{C2} is the voltage of capacitor C_2.

2) Second Stage (t_1, t_2): At the moment of t_1, the switch S_1 is turned ON, the inductor L_1 starts to store energy from zero as shown in Fig.3(b). In the meantime, if (V_{C1} + V_{C2}) $\prec V_O$, where V_{C1} is the capacitor C_1 voltage, the diode D_2 will be turned OFF and the diode D_{M2} will be turned ON; therefore, the energy in the inductor L_2 will be transferred to the capacitor $C1$. If there is enough energy in the inductor L_2, V_{C1} will be charged to the following state: V_{C1} + $V_{C2} \geq V_O$. Then, the diode D_2 will be turned ON again, which is shown in Fig.5. If there is not enough energy to charge VC 1 to (V_O – V_{C2}), then

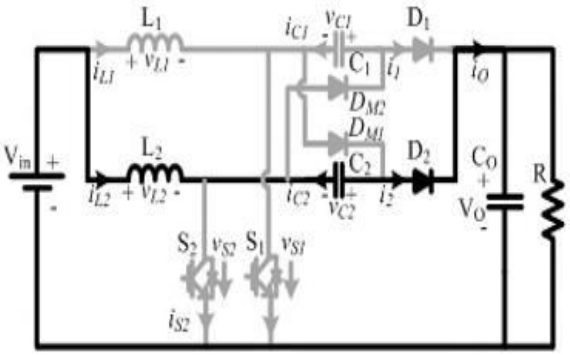

(a)

International Journal for Innovative Engineering and Management Research
A Peer Revieved Open Access International Journal
www.ijiemr.org

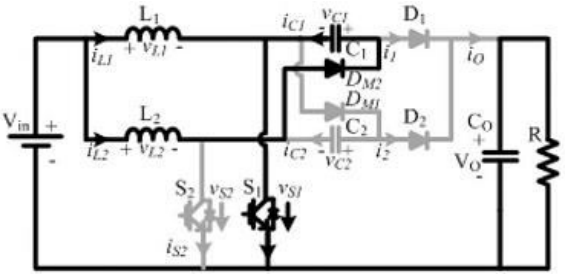

(b)

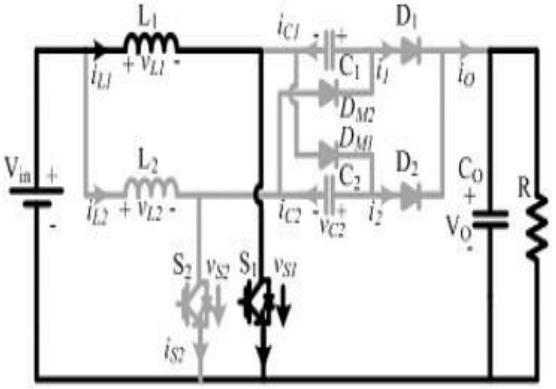

(c)

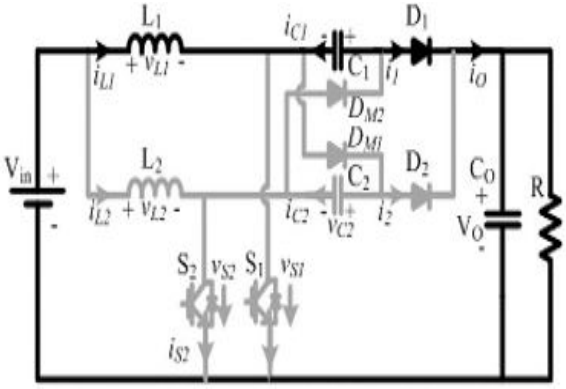

(d)

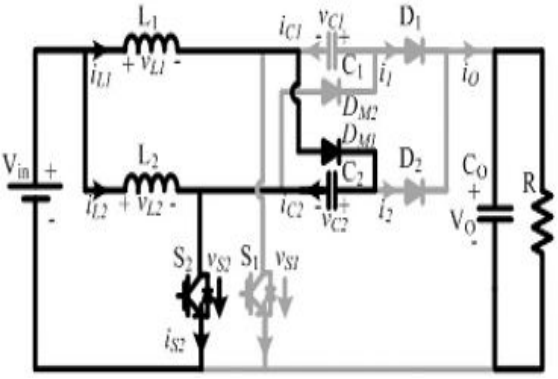

(e)

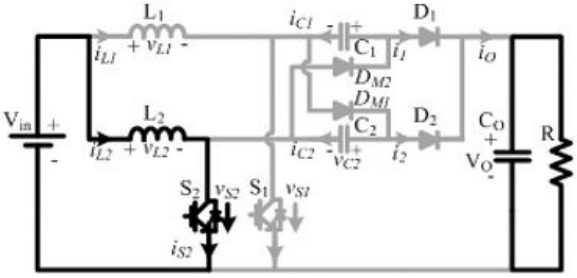

(f)

Fig.3. Stages at boundary condition. (a) First stage (t0, t1), (b) second stage (t1, t2), (c) third stage (t2, t3), (d) fourth stage (t3, t4), (e) fifth stage (t4, t5), (f) sixth stage (t5, t6).

it will come to the Third Stage as shown in Fig.3(c). If the energy in the inductor L_2 is just discharged to zero and $V_{C1} + V_{C2} = V_O$ at the end of the stage, then we say that the circuit operates in the boundary condition state. During the stage, the voltage stress-on switch S_2 is $V_{C\ 1}$.

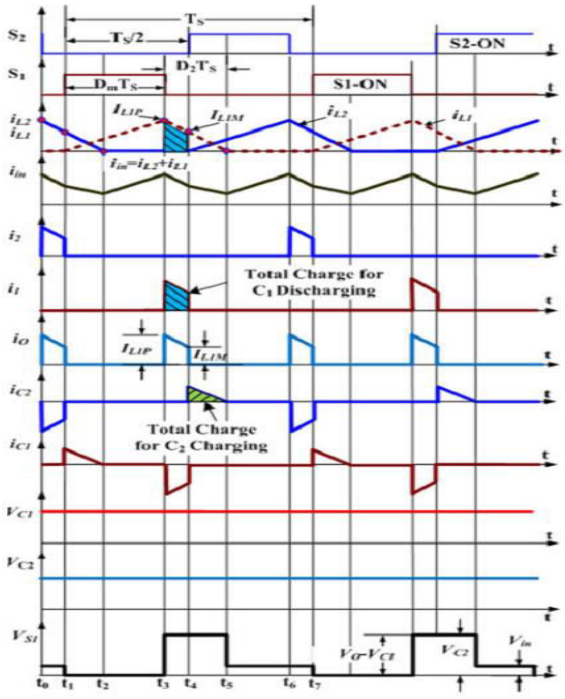

Fig.4. Main theoretical waveforms at boundary condition

International Journal for Innovative Engineering and Management Research
A Peer Revieved Open Access International Journal
www.ijiemr.org

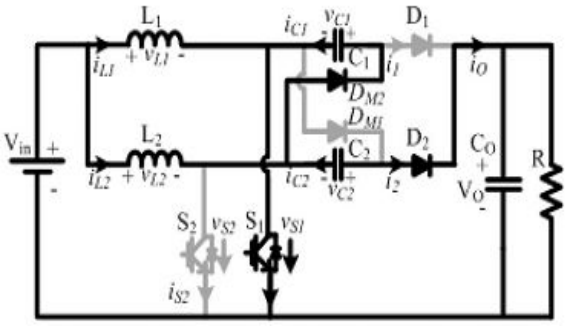

Fig.5. One stage above boundary condition

3) Third Stage (t_2,t_3): At the moment of t_2, the current in the inductor L_2 just falls to zero, all the diodes are in off state and the inductor L_1 is in charging state until the switch S_1 is turned OFF at the moment of t_3. The voltage stress on switch S_2 is Vin. At the end of this stage, the current in the inductor L_1 comes to the peak value I_{L1P}, and

$$I_{L1P} = \frac{V_{\text{in}} D_m T_S}{L} \tag{1}$$

where Vin is the input voltage, L is the inductance of L_1 and L_2,Dm is the duty cycle at boundary condition, and T_S is the switching period.

4) Fourth Stage (t_3, t_4): At the moment of t_3, switch S_1 and S_2 are in off state, the energy in the inductor L_1 and the capacitor C_1 will be transferred to the output capacitor C_O through the diode D_1, which is similar to First Stage. In this stage, the voltage stress on switch S1 is $(V_O - V_{C1})$, and the voltage stress on switch S_2 is Vin. At the end of this stage, the current in the inductor L_1 decreases to be I_{L1M}

$$I_{L1M} = I_{L1P} - \frac{V_O - V_{C1} - V_{\text{in}}}{L}(0.5 - D_m)T_S \tag{2}$$

5) Fifth Stage (t_4, t_5): At the moment of t_4, the switch S2 is turned ON and the inductor L_2 starts to store energy. This stage is similar to the Second Stage. In this stage, the voltage stress on switch S_1 is V_{C2}. At the end of this stage, the current in the inductor L_1 decreases to zero from I_{L1M}. And thus

$$I_{L1M} - \frac{V_{C2} - V_{\text{in}}}{L}(D_2 - 0.5 + D_m)T_S = 0 \tag{3}$$

where D_2 is the duty cycle as shown in Fig.4.

6) Sixth Stage (t_5, t_6): At the moment of t_5, the current in the inductor L_1 decreases to zero. All the diodes are in off state and the inductor L_2 is in charging state until the stage comes to the end at the moment t_6. A new switching period will begin with the next First Stage.From the aforementioned analysis, the voltage sum of capacitor C_1 and C_2 will be V_O at boundary condition. If it is less than V_O, the voltage stress on switch S_1 and S_2 will be larger than $V_O/2$, because the voltage stress on switch S1 is $(V_O - V_{C1})$ during the Fourth Stage and the voltage stress on switch S_2 is $(V_O - V_{C2})$ during the First Stage.The average value of the output current i_O is equal to the dc component of the load current V_O/R, then

$$\frac{V_O}{R} = \frac{1}{T_S}\int_0^{T_S} i_O dt = \frac{1}{T_S}\int_0^{T_S} (i_1 + i_2)dt$$

$$= \frac{1}{T_S}\int_0^{T_S} i_1 dt + \frac{1}{T_S}\int_0^{T_S} i_2 dt \tag{4}$$

International Journal for Innovative Engineering and Management Research
A Peer Revieved Open Access International Journal
www.ijiemr.org

Considering the same parameters of the circuit in two phases as shown in Fig.2, therefore

$$\frac{1}{T_S}\int_0^{T_S} i_1 dt = \frac{1}{T_S}\int_0^{T_S} i_2 dt. \tag{5}$$

By combining (4) and (5), it is derived

$$\frac{V_O}{R} = \frac{2}{T_S}\int_0^{T_S} i_1 dt = \frac{2}{T_S}\int_{t3}^{t4} i_1 dt$$

$$= \frac{2}{T_S}\cdot\left[\frac{1}{2}(I_{L1P}+I_{L1M})(0.5-D_m)T_S\right]$$

$$= (I_{L1P}+I_{L1M})(0.5-D_m) \tag{6}$$

where R is the load.

At the boundary condition, the diode D2 (D1) approaches the conduction state during the Second Stage (Fifth Stage), which is shown in Fig.5.

The following equation can be obtained

$$V_{C1}+V_{C2}=V_O \tag{7}$$

Considering both capacitors C1 and C2 are large enough, average voltage of the capacitor will keep equal. Otherwise, the converter will not operate at boundary condition, therefore

$$V_{C1}=V_{C2}=\frac{1}{2}V_O \tag{8}$$

By substituting (1) and (8) into (2), the current I_{L1M} can be derived

$$I_{L1M}=\frac{V_{\text{in}}-V_O/2+V_O\cdot D_m}{2L}T_S \tag{9}$$

As shown in Fig.4, the total discharge of capacitor C_1 between t_3 and t_4 is

$$Q_{C1}=\int_{t_3}^{t_4} i_{L1}dt=\frac{1}{2}(I_{L1P}+I_{L1M})(0.5-D_m)T_S \tag{10}$$

The total charge of capacitor C_2 between t_4 and t_5 is

$$Q_{C2}=\int_{t_4}^{t_5} i_{L1}dt=\frac{1}{2}I_{L1M}(D_2-0.5+D_m)T_S \tag{11}$$

According to the previous analysis, the total discharge of C_1 is equal to the total charge of capacitor C_2 at boundary condition. Therefore, there will be

$$Q_{C1}=Q_{C2} \tag{12}$$

By combining (10), (11), and (12), the following can be de rived

$$D_2=(0.5-D_m)\left(\frac{I_{L1P}}{I_{L1M}}+2\right) \tag{13}$$

By combining (3) and (6) and then substituting (1), (9), and (13) into them, the boundary condition can be derived as

$$\begin{cases} K=K\text{crit}=\dfrac{n-2}{2n(n-\sqrt{2})^2} & (a)\\ D_m=\dfrac{n-2}{2(n-\sqrt{2})} & (b)\end{cases} \tag{14}$$

where n is the voltage gain of the converter (n = VO/Vin), and K is the parameters of the circuit and K = 2L/(R × TS).

The boundary constraint with traditional interleaving control decided by (14) is shown in Fig.6. The constraint includes two parts: duty cycle D and the circuit parameters K = 2L/(R × TS).

As the switching period TS and the input inductor L are designed at nominal operation in continuous conduction mode

International Journal for Innovative Engineering and Management Research
A Peer Revieved Open Access International Journal
www.ijiemr.org

(CCM), the constraint is determined by duty cycle D and the load R. The reason why there are two parts in the boundary constraint is that the duty cycle D varies with the load when the converter operates in DCM. For a given application, the voltage gain of the dc/dc converter is determined. And then, the minimum duty cycle that can maintain low-voltage stress in main power devices with traditional interleaving control will be given by (14)-(b) and as shown in Fig.6(a). At the same minimum duty cycle, the converter operates at boundary condition when the circuit parameters K = 2L/(R × TS) satisfy (14)-(a) and as shown in Fig.6(b).When the converter operates above the boundary condition, the circuit parameters are in Zone A of Fig.6(b), i.e.,K > Kcrit, the converter could achieve halved voltage stress on switches with traditional interleaving control with the duty cycle above the solid red line as shown in Fig.6(a). When decreasing the load to the solid red line at boundary condition in Fig.6 (b), i.e., K = Kcrit, the duty cycle of the converter will be decreased to the solid red line in Fig.6(a). When decreasing the load further in Zone B in Fig.6(b), i.e., K < Kcrit, the duty cycle will be decreased further to be smaller than the minimum duty cycle that maintains low-voltage stress on switches with traditional interleaving control. Then, the APS control should be used to achieve halved voltage stress on switches in Zone B.

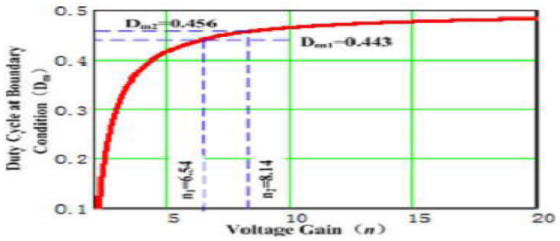

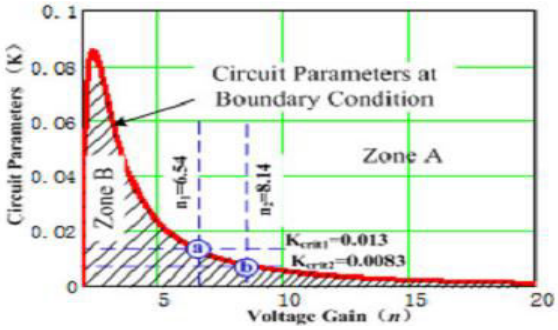

(b)

Fig.6. Boundary constraint varies with voltage gain. (a) Duty cycle at boundary condition varies with voltage gain, (b) circuit parameters at boundary condition varies with voltage gain.

3.3 Control Scheme of All Power Range with Aps And Traditional Interleaving Control

According to the principle of APS, APS control is proposed to solve the light load problem with duty cycle less than 0.5 as shown in Fig.7(a). With the load increasing, the duty cycle will be increased as well. When the duty cycle is increased to 0.5, the APS control will be altered to be traditional interleaving control with halved switching frequency as shown in Fig.7(b).

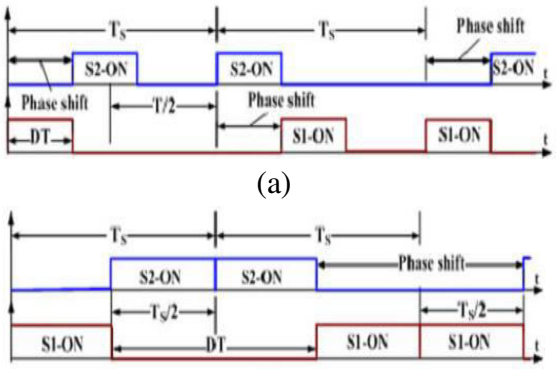

(a)

(b)

Fig.7. PWM waveform of APS with D < 0.5 and D = 0.5. (a) D < 0.5, (b) D = 0.5.

International Journal for Innovative Engineering and Management Research
A Peer Revieved Open Access International Journal
www.ijiemr.org

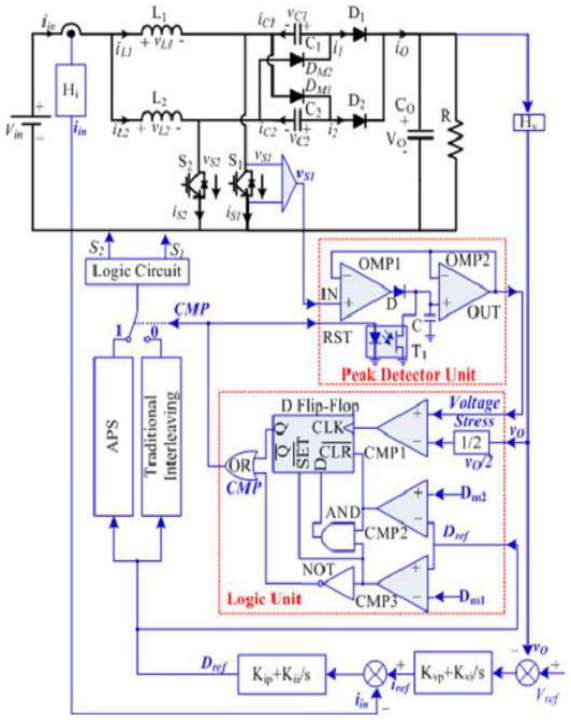

Fig.8. Block diagram of the converter with the control scheme of all power range

According to previous analysis as shown in Fig.6, the minimum duty cycle to achieve low-voltage stress on switches with traditional interleaving control is less than 0.5. Therefore, it is possible to combine both APS control and traditional interleaving control to control the converter for full power range operation.

Table I

Operational Principle of the Logic Unit in Fig.8

$v_{S1}>0.5v_O$	$D_{ref}>D_{m1}$	$D_{ref}<D_{m2}$	Control Method
X	1	0	Traditional interleaving control
X	0	1	APS control
0	1	1	Keep the previous control mode
1	1	1	Swap from traditional interleaving control to APS control and stay in APS control until $D_{ref}>D_{m2}$

The control scheme is shown in Fig.8. The duty cycle is divided into three areas: D < Dm1,D > Dm2, and Dm1 ≤ D ≤ Dm2. In the first area, i.e., D < Dm1, APS control will be used because traditional interleaving control cannot be effective to maintain low-voltage stress on switches. In the second area, i.e., D > Dm2, traditional interleaving control will be used. In the third area, i.e., Dm1 ≤ D ≤ Dm2, either APS control or traditional interleaving control may be used.In the first area (D < Dm1) with APS control and the second area (D > Dm2) with traditional interleaving control, the capacitor voltage is half of the output voltage. Therefore, the switches voltage stress is clamped to half of the output voltage.The swapping between the APS control and traditional interleaving control in the area Dm1 ≤ D ≤ Dm2 is achieved by detecting the voltage stress of the switch S1 as shown in Fig.8. When the voltage stress of the switch S1 is higher than half of the output voltage, the control is changed from interleaving control to APS control. If the traditional interleaving control is initially used in the second area (Dm1 ≤ D ≤ Dm2) and once the switch S1 voltage stress is larger than half of the output voltage, the logic unit output CMP in Fig.8 will be changed to CMP = 1 and APS control will be enabled. The aforementioned function for swapping between the APS and traditional interleaving control is achieved by the Logic Unit as shown in Fig.8, and the operational principle of the Logic Unit is shown in Table 1.If APS control mode is used (i.e., CMP = 1), the optocoupler transistor T1 is turned ON, the voltage of capacitor C in the peak detector unit is

International Journal for Innovative Engineering and Management Research
A Peer Revieved Open Access International Journal
www.ijiemr.org

resetted and the peak detector unit is disenabled. If the traditional interleaving control mode is used (i.e., CMP = 0), the optocoupler transistor T1 will be turned OFF, and the peak detector unit is enabled and used to detect the voltage stress of switch S1.In order to achieve better dynamic performance operation, dual loop control is adopted as shown in Fig.8, in which the inner current loop is to control the input inductor current while the outer voltage loop is to control the output voltage. Kip and Kii are the PI controller parameters of the inner current loop, while Kvp and Kvi are the PI controller parameters of the outer voltage loop.

V. INDUCTION MOTOR

In recent years the control of high performance induction motor drives for general industry applications and production automation has received widespread research interests. Induction machine modeling has continuously attracted the attention of researchers not only because such machines are made and used in largest numbers but also due to their varied modes of operation both under steady and dynamic states. Traditionally, DC motors were the work horses for the Adjustable Speed Drives (ASDs) due to their excellent speed and torque response. But, they have the inherent disadvantage of commutator and mechanical brushes, which undergo wear and tear with the passage of time. In most cases, AC motors are preferred to DC motors, in particular, an induction motor due to its low cost, low maintenance, lower weight, higher efficiency, improved ruggedness and reliability. All these features make the use of induction motors a mandatory in many areas of industrial applications. The advancement in Power electronics and semiconductor technology has triggered the development of high power and high speed semiconductor devices in order to achieve a smooth, continuous and low total harmonics distortion (THD). Three phase induction motors are commonly used in many industries and they have three phase stator and rotor windings. The stator windings are supplied with balanced three phase ac voltages, which produce induced voltages in the rotor windings due to transformer action. It is possible to arrange the distribution of stator windings so that there is an effect of multiple poles, producing several cycles of magneto motive force (mmf) around the air gap. This field establishes a spatially distributed sinusoidal flux density in the air gap. In this paper three phase induction motor as a load. The equivalent circuit for one phase of the rotor is shown in figure.9.

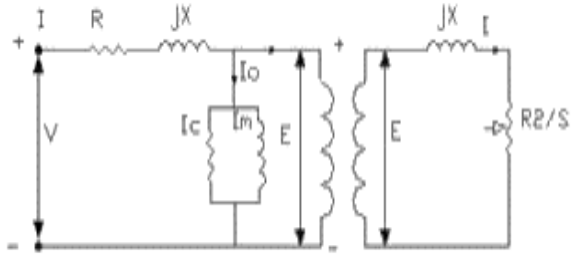

Fig.9. Steady state Equivalent circuit of an induction Motor.

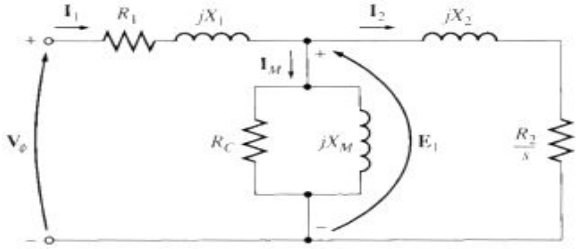

Fig.10. Equivalent circuit refer to stator.

The rotor current is

International Journal for Innovative Engineering and Management Research
A Peer Revieved Open Access International Journal
www.ijiemr.org

$$I_r = \frac{sE_r}{R_r + jX_r} = \frac{E_r}{\frac{R_r}{s} + jX}$$

VI.MATLAB/SIMULATION RESULTS

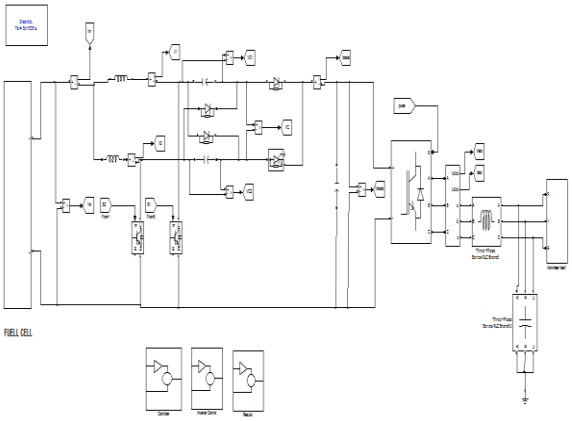

Fig.11. Simulink model of proposed system under nonlinear loads

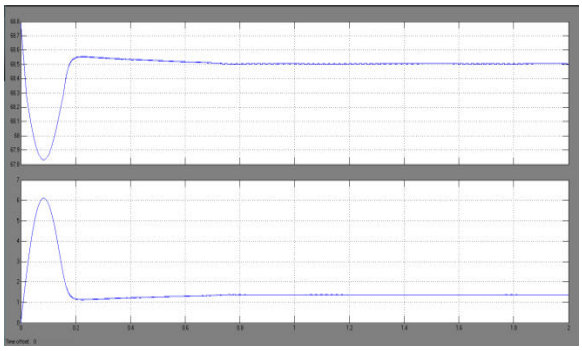

Fig.12. Simulation waveforms for Fuel cell voltage and current

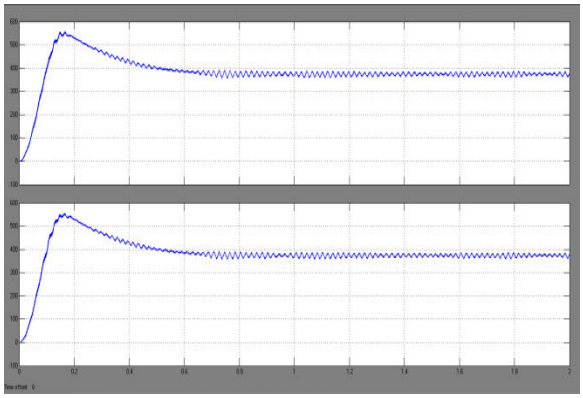

Fig.13. Simulation waveform for two-phase interleaved boost converter with voltage multiplier Capacitor voltages Vc_1, Vc_2

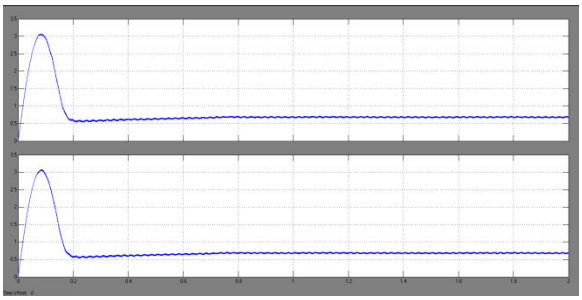

Fig.14. Simulation waveforms for Current Sources IL1,IL2 at series of high step converter

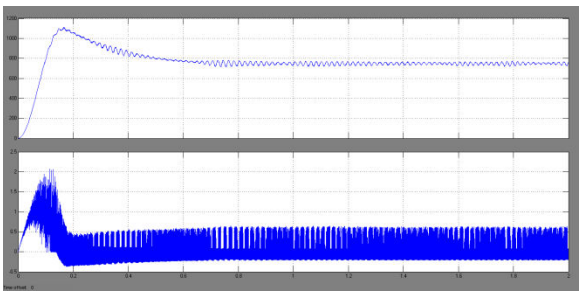

Fig.15. Simulation waveforms for Boost Voltage and Boost current

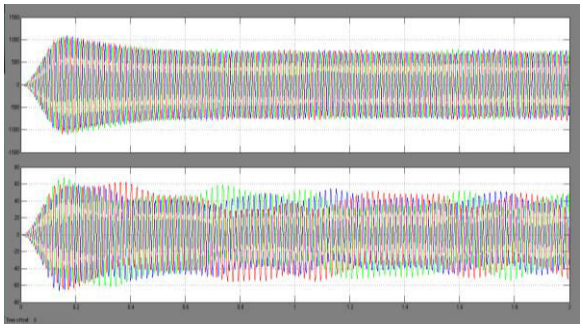

Fig.16. Simulation waveforms for Phase voltages (Vabc) and Phase currents Iabc from inverter

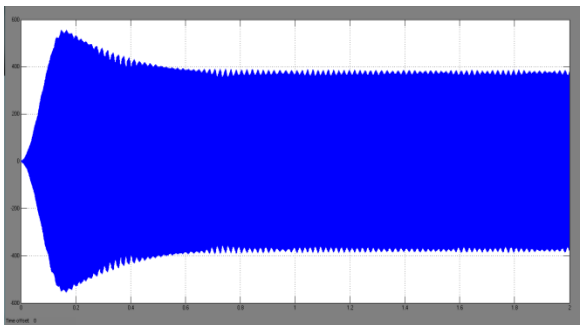

Fig.17. Simulation waveform for Capacitor Voltage (Vc)

International Journal for Innovative Engineering and Management Research
A Peer Revieved Open Access International Journal
www.ijiemr.org

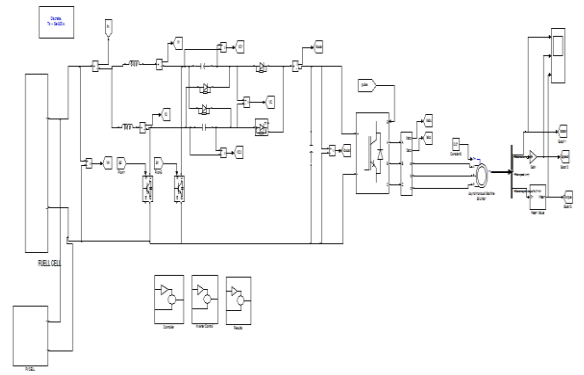

Fig.18. Grid-connected power system based on fuel cell with Induction Motor Drive

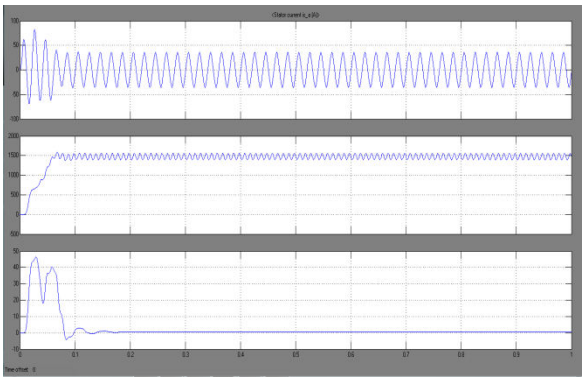

Fig.19. Simulation waveform for Grid-connected power system based on fuel cell with Induction Motor Drive Stator current, speed and Electromagnetic Torque

VIII.CONCLUSION

In this work the boundary condition is derived after stage analysis in this project. The boundary condition classifies the operating states into two zones, i.e., Zone A and Zone B. The traditional interleaving control is used in Zone A while APS control is used in Zone B. And the swapping function is achieved by a logic unit. With the proposed control scheme, the converter can achieve low voltage stress on switches in all power range of the load. By connecting induction motor to the proposed system the performance in case of stator current, speed and electromagnetic torques are observe to be better.

REFERENCES

[1] Mr. Lili Kumar Uttarala, Dr. J. Viswanatha Rao, Mr. Kranthi Kumar. Vanukuru and Mrs. Battula Asha Kiran, "Res Fed High Gain Dc-Dc Converter with Closed Loop Control for Induction Motor Drive," International conference on Signal Processing, Communication, Power and Embedded System (SCOPES)-2016.

[2] Minsoo Jang, Mihai Ciobotaru, "A Single-Phase Grid-Connected Fuel Cell System Based on a Boost-Inverter," IEEE transactions on power electronics, vol. 28, no. 1, january 2013.

[3] T.N.V.T.Sahiteesh, K.Madhu Krishna, "Single Phase Induction Motor Fed with High Step-Up Converter Based PV Solar System," SSRG International Journal of Electrical and Electronics Engineering (SSRG-IJEEE) – volume 2 Issue 1 Jan 2015.

[4] G. Fontes, C. Turpin, S. Astier, and T. A. Meynard, "Interactions between fuel cells and power converters: Influence of current harmonics on a fuel cell stack," IEEE Trans. Power Electron., vol. 22, no. 2, pp. 670–678, Mar. 2007.

[5] S. Wang, Y. Kenarangui, and B. Fahimi, "Impact of boost converter switch ing frequency on optimal operation of fuel cell systems," in Proc. IEEE Vehicle Power Propulsion Conf., 2006, pp. 1–5.

[6] P. Thounthong, B. Davat, S. Rael, and P. Sethakul, "Fuel starvation," IEEE Ind. Appl. Mag., vol. 15, no. 4, pp. 52–59, Jul./Aug. 2009.

[7] L. Wuhua, F. Lingli, Z. Yi, H. Xiangning, X. Dewei, and W. Bin, "High

step-up and high-efficiency fuel-cell power-generation system with active clamp flyback-forward converter," IEEE Trans. Ind. Electron., vol. 59, no. 1, pp. 599–610, Jan. 2012.

[8] S. K. Mazumder, R. K. Burra, and K. Acharya, "A ripple-mitigating and energy-efficient fuel cell power-conditioning system," IEEE Trans. Power Electron., vol. 22, no. 4, pp. 1437–1452, Jul. 2007.

[9] Z. Qun and F. C. Lee, "High-efficiency, high step-up DC–DC converters," IEEE Trans. Power Electron., vol. 18, no. 1, pp. 65–73, Jan. 2003.

[10] B. Axelrod, Y. Berkovich, and A. Ioinovici, "Switched-capacitor/ switched-inductor structures for getting transformerless hybrid DC–DC PWM converters," IEEE Trans. Circuits Syst. I: Reg. Papers, vol. 55, no. 2, pp. 687–696, Mar. 2008.

[11] Y. Changwoo, K. Joongeun, and C. Sewan, "Multiphase DC–DC converters using a boost-half-bridge cell for high-voltage and high-power applications," IEEE Trans. Power Electron., vol. 26, no. 2, pp. 381–388, Feb. 2011.

[12] H. Yi-Ping, C. Jiann-Fuh, L. Tsorng-Juu, and Y. Lung-Sheng, "A novel high step-up DC–DC converter for a microgrid system," IEEE Trans. Power Electron., vol. 26, no. 4, pp. 1127–1136, Apr. 2011.